SCIEPublish

Article

Reactions and Phase Transformations at Sintering of Cubic Boron Nitride Based Materials

Stepan Pavlov [1], Andrey Yurkov [1,*] and Mikhail Andrianov [2]

[1] Department of Chemical Technology of Ceramics and Refractories of Mendeleev Chemical Technological University of Russia, 125047 Moscow, Russia; stepanpahome@gmail.com (S.P.)

[2] Microbor LLC, 109316 Moscow, Russia; mandrianov@microbor.com (M.A.)

* Corresponding author. E-mail: and-yur@mail.ru or Yurkov.a.l@muctr.ru (A.Y.)

Received: 13 August 2024; Accepted: 26 September 2024; Available online: 29 September 2024

ABSTRACT: Superhard cubic boron nitride (cBN) cutting materials with different contents of cBN were investigated. The compositions of cBN-based materials included ceramic and metallic binders. The sintering of materials was performed by high-temperature hot pressing (HPHT) six-anvil apparatus at pressure 4.5 GPa and temperatures 1400–1450 °C. The process of compaction and processing of superhard cBN materials is followed by numerous chemical reactions. The chemical reactions are very important in compaction and sintering. The volume transformations during chemical reactions affect the shrinkage of the materials and may also impact the residual porosity of the finished products. The adhesion between the grains also depends on these chemical reactions. The research analyzed the volume transformations of various reactions during HPHT sintering of cBN materials, which may play a significant role in forming their structure and properties.

Keywords: Cubic boron nitride; Volume transformations; Reactions; Phase composition

1. Introduction

Cubic boron nitride (cBN) materials are widely used to cut iron-based hard alloys because cBN is stable in air up to 1200 °C and is inert in contact with ferrous alloys [1].

The application of cBN materials of boron high (BH), boron low (BL) and boron coated (BC) groups [2] is different. Metallic and ceramic binders may be used to process cBN materials. Metallic binders heat is conductive and fracture resistant but have rather low temperature softening points. Ceramic binders are hard and stable at high temperatures but are brittle and less heat conductive.

Oxidation in machining by cBN cutting tools is one of the mechanisms of deterioration of properties of cutting tools—alongside abrasion, adhesion, and diffusion—which govern tool deterioration [3]. The application of ceramic binders to cBN materials is an effective approach to improve oxidation and diffusion.

Yet the additions of ceramic binders are followed by deterioration of mechanical properties. This is why cBN cutting tools with high content of binders (and low content of cBN) are used for continuous final cutting (low mechanical loads and high temperatures.

The wear of the cutting tool is a very complex process. The temperatures of the process are very high, the wear includes adhesion and diffusion, and the cyclic stresses during the wear process are close to strength characteristics. The wear of cutting tools is very difficult for modelling and simulations.

The application of cBN cutting tools depends on the content and the types of binders. There are BL and BH groups of cBN cutting tools. The materials of the BH group (below 20% of metallic and ceramic binders (Ni, Co, AlN, AlB_{12}) are used for rough, non-continuous cutting due to high fracture toughness and hardness [4,5]. The materials of the BL group (30–70% of metallic and ceramic binders) are used for continuous finishing cutting [6].

There are many substances used as binders. However, the most popular (and well-investigated) are the materials of the BL group with titanium compounds—TiN, TiC and Ti(C, N) [7].

https://doi.org/10.70322/htm.2024.10006

There is information that the best workability at finishing cutting of Inconel 718 at the speed 200–300 m/min was by BL cBN cutting tool with titanium compounds (TiN, TiC and Ti(C, N)) as binders and fine cBN grains [8].

The sequence of wear mechanisms in cBN tools for cutting metals is adhesion, diffusion and abrasion due to friction. J. P. Costes et al. suggest that an increase of cBN content from 60% to 80% decreases cutting service time of a cutting tool from 9.6 min to 2.8 min [8].

Metallic binders are aluminum, tungsten, molybdenum, cobalt, nickel, zirconium and others [9]; ceramic binders are carbides of transition IV group metals—titanium boride, aluminum nitride, titanium nitride, titanium carbonitride [10–12]. Aluminum has the lowest melting temperature, is reactive and has a low viscosity.

The processing of cBN materials during sintering at multi-anvil compression is followed by chemical reactions and phase transformations of components.

Metallic aluminum is often used as a binder for cBN. At 660 °C, aluminum melts, filling the spaces between cBN grains while promoting densification under applied pressure.

The reactions may occur [5] between aluminum and boron nitride. The reaction products are new ceramic compounds aluminum nitride AlN and aluminum boride AlB_{12}. These substances have rather high Young modulus and hardness. However, the adhesion between grains of cBN and the newly appeared substances, even at pressure during sintering, needs additional investigations. Titanium, which is also added to the starting mix, is rather reactive. It reacts with cBN to form titanium nitride TiN and titanium boride TiB_2. Titanium nitride and titanium boride are hard and thermally stable substances [10].

The research aims to analyze the chemical reactions between the components of cBN-based materials and to calculate the volume transformations (volume effects) during chemical reactions in the HPHT fabrication of cBN materials with both high and low contents of metallic and ceramic binders.

2. Materials and Methods

The average grain size of the starting cubic boron nitride powder was 1–3 μm, and the purity −99.5%. Commercially available Al, Mo, TiC, TiN were also used in this research. Two groups of materials were synthesized and investigated, one with a high content of cBN and the other with a low content.

The materials with low cBN content (BL–group) contained more than 45 vol. % cBN. The other components in the starting mixtures were Al, TiC, TiN and molybdenum. The materials with high cBN content (BH–group), contained more than 70 vol. % cBN; the other components were Al and TiC.

The cutting materials (SNGN 1204 blades) were made with industrial equipment. The initial powders were mixed in the form of a liquid slurry. Then the resulting suspension was dried in a spray dryer to obtain aggregation-stable spherical particles (granules) (Figure 1), conglomerates from a mixture of raw materials introduced into the charge.

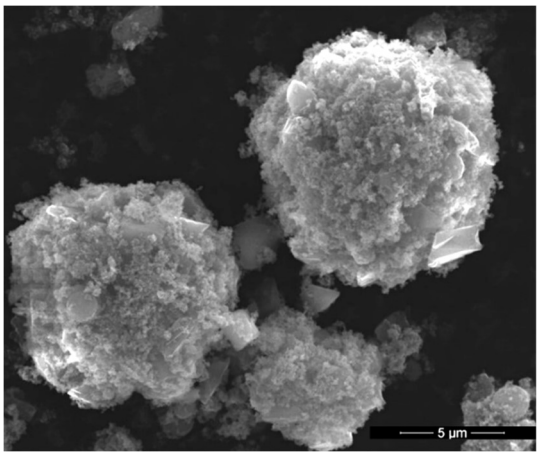

Figure 1. Granules of starting mix after drying. 10,000×.

Ultrasonic mixing with a selected plasticizer and drying conditions (Figure 1) gives uniform granules of cBN-based mix for future six-anvil pressing.

The pre-shapes 36 × 22 mm were compacted at pressure 420 MPa. The sintering HPHT process was fulfilled at a six-anvil apparatus in a pyrophyllite container at pressure 4.5 GPa and temperature 1400–1450 °C for 5 min.

The open porosity and apparent density of the materials were determined according to ISO 5017:2013-01 [13].

The shaped compacts were cut by electro-erosion into special shapes for future investigations.

The Vickers hardness was determined on Durascan g20 hardness tester at loads 0.5; 1; 2; 2.5; 3 and 5 kgf (the application of load 15 seconds). The image of the imprint after indentation at loads 5 kgf is shown in Figure 2. The specimens were 25 mm in diameter and 3.15 mm high. Vickers hardness was calculated according to the standard equation:

$$H_v = 1.8544 \frac{P}{d^2}, \quad (1)$$

where P—is load and d is diagonal of indent.

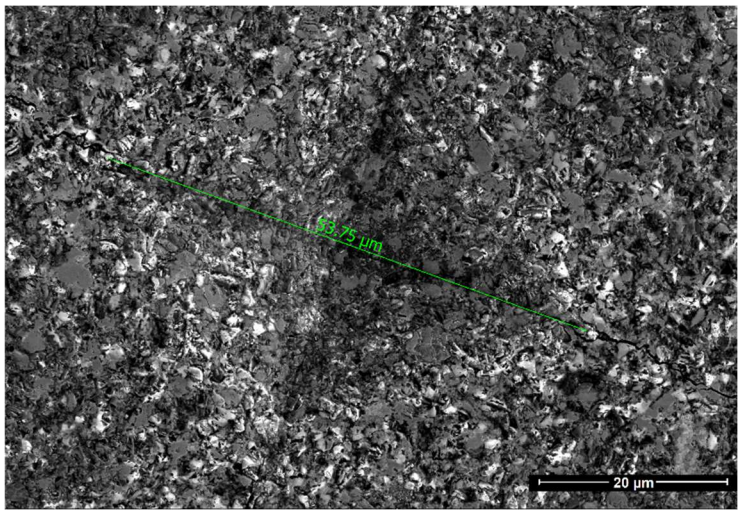

Figure 2. The indents in cBN BL specimen at loads 5 kgf.

The fracture toughness was calculated according to Niihara Equation (2) [14–16].

$$K_{Ic} = 0.034 \left(\frac{E}{H}\right)^{0.4} \frac{P}{c^{1.5}}, \quad (2)$$

where E—Young modulus (GPa), H is hardness, P is load and c is half of the crack length.

Structures were analyzed with the help of scanning electron microscope Helios NanoLab 650 in BSE regime, XRD analysis was made by Genesis Apex Energy Dispersive Spectroscopy System. XRD analysis was made on D8 Advance AXS (Bruker, Billerica, MA, USA), CuKα, λ = 1.5418 Å, 0.2°/min, 2Θ 20–80°, DIFFRACplus EVA и DIFFRACplus SEARCH were used for the calculations.

3. Results

The materials of the BL group and BH group have different structures (Figure 3), which is obvious because the concentration of the main phase in the materials of BL group and BH group differ.

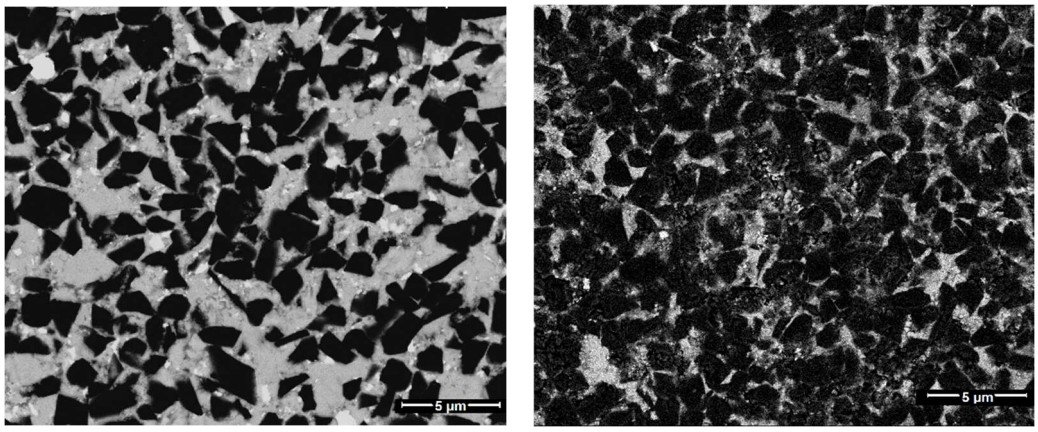

(**a**) (**b**)

Figure 3. The structures of material: (**a**) with low cBN content (BL group) and with (**b**) high cBN content (BH group).

The residual porosity of the BH and BL series sintered materials in our research is approximately the same and can be considered quite low. We didn't detect the pores on SEM images (Figure 3), probably because the porosity values

are small. However, the lack of pores in the SEM images may indicate that the dimensions of the residual pores are small and significantly smaller than the dimensions of the material grains.

The tested Vickers hardness values demonstrate rather high values for the specimen of BH group and moderate values for the specimen of the BL group.

During hardness testing, we observed the "indentation size effect"—the hardness values at low loads are significantly lower compared to those at high loads [17]. It is considered that in the materials without (or almost without porosity) and with uniform structure, the load dependence of hardness reaches a plateau. At high loads, the hardness becomes constant. In our case, at the specimen of BH group, the value of hardness at 2 kgf was 61.65 GPa, while at 5 kgf it was 41.7 GPa. For BL group, the value of hardness at 2 kgf was 48.7 GPa, while at 5 kgf it was 37.3 GPa. The hardness values at 5 kgf are in Table 1. Our results suggest that the real hardness values of cBN materials may be obtained only at high loads on the indenter (5 kgf).

The difference between the fracture toughness values for cBN materials of BL and BH groups is lower. Still, we see (Table 1) 7.6 ± 0.5 MPa·$m^{0.5}$ for the BH group and 6.4 ± 0.5 MPa·$m^{0.5}$ for BL group.

Table 1. The properties of investigated materials of BH and BL groups.

Specimen	Apparent Density, g/cm^3	Open Porosity, %	Shrinkage, %	H_V, GPa (load)	K_{IC}, MPa·$m^{0.5}$
BH–group	3.518	1.01	37.8	61.65 ± 2	7.6 ± 0.5
BL–group	4.067	1.29	32.2	48.7 ± 2	6.4 ± 0.5

The sintering HPHT process is accompanied by chemical reactions. Both starting mixtures contain considerable amount of aluminum, yet XRD analysis (Figure 4a,b) shows no free aluminum in specimen of both groups.

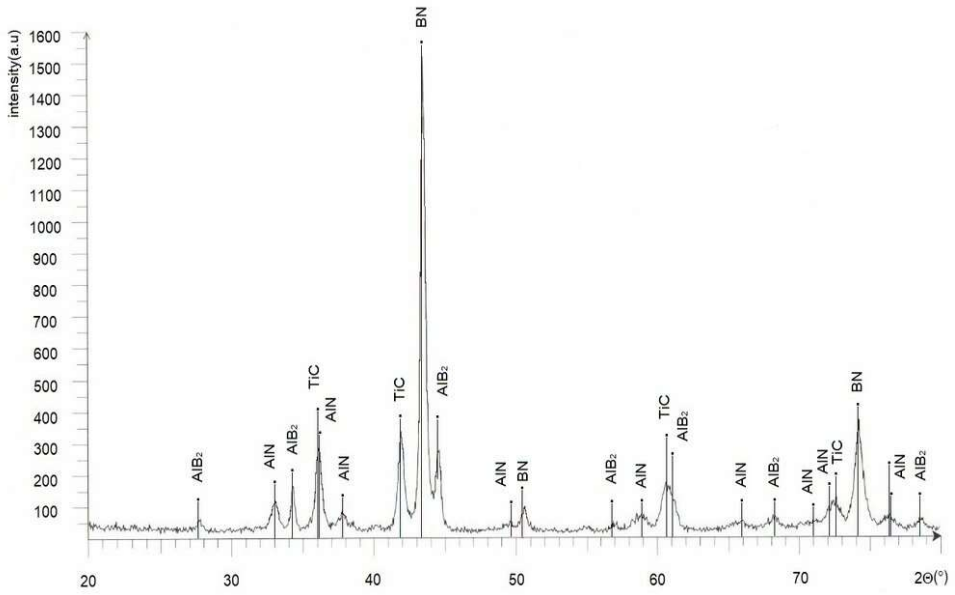

(**a**)

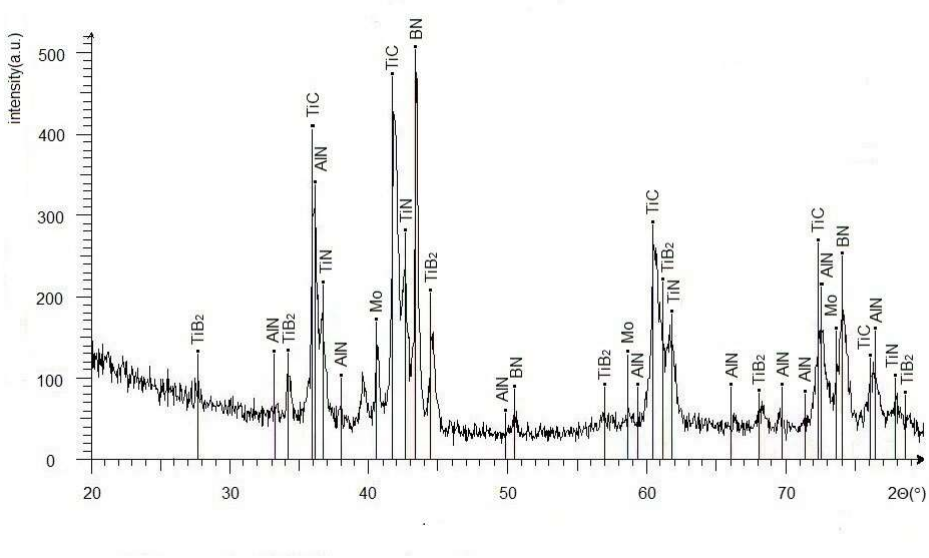

(**b**)

Figure 4. X-ray diffractograms of specimen of (**a**) BH and (**b**) BL groups.

We can see the presence of TiC, AlN, and AlB_2 in the sintered specimen of the BH group. In the sintered specimen of the BL group, there is aluminum nitride, titanium boride and titanium carbide, but molybdenum is unreacted, and there are no traces of molybdenum-containing compounds.

Chemical compositions of selected areas of cBN based material (BL group) are in Table 2. We can see compositions of grains (according to EDX spectroscopy) that may be attributed to titanium nitride, titanium nitride carbide, aluminum nitride. Molybdenum is in unreacted form (the grains of unreacted molybdenum) and in reacted forms (molybdenum boride and molybdenum carbide).

Table 2. EDX mapping of the surface of the specimen (Figure 5) and selected spots with compositions.

Spectrum	EDS Spot 1		EDS Spot 2		EDS Spot 3	
	wt. %	at. %	wt. %	at. %	wt. %	at. %
B	22.53	29.01	26.64	55.77	0.5	1.31
C	14.93	17.30	5.11	9.62	3.71	8.67
N	50.09	49.77	6.97	11.26	6.19	12.41
O	-	-	4.00	5.65	21.93	38.50
Ti	10.33	3.00	14.65	6.92	64.28	37.69
Mo	0.40	0.03	41.46	9.78	2.83	0.83
Al	1.73	0.89	1.18	0.99	0.56	0.59
Σ	100	100	100	100	100	100

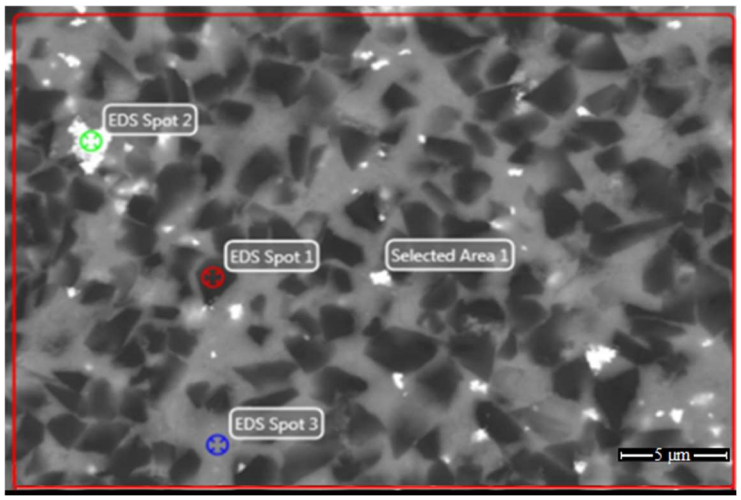

Figure 5. The areas of EDX analysis (Table 2) on the surface of cBN material (BL group).

The specimen of BL and BH groups were tested for grinding on steel disk (HRC 68–69, Rz = 3.4–3.7 μm, d = 105 mm) (Figure 3). The results of fine grinding (with stroke) are in Table 3. The wear of the cutting tools of BL composition is 83 μm (Figure 6a), and the wear of the plates of BH composition is 68 μm (Figure 6b).

Table 3. The results of fine lengthwise grinding (with stroke) with test cutting materials of BL and BH group.

Test Cutting Material	Grinded Material	Hardness, HRC	Turning Mode			Wear, μm
			V, m/min	S, mm/r	t, min	
BL	steel (GCr15)	68–69	120	0.1	3	83
BH	steel (GCr15)	68–69	180	0.3	1.5	68

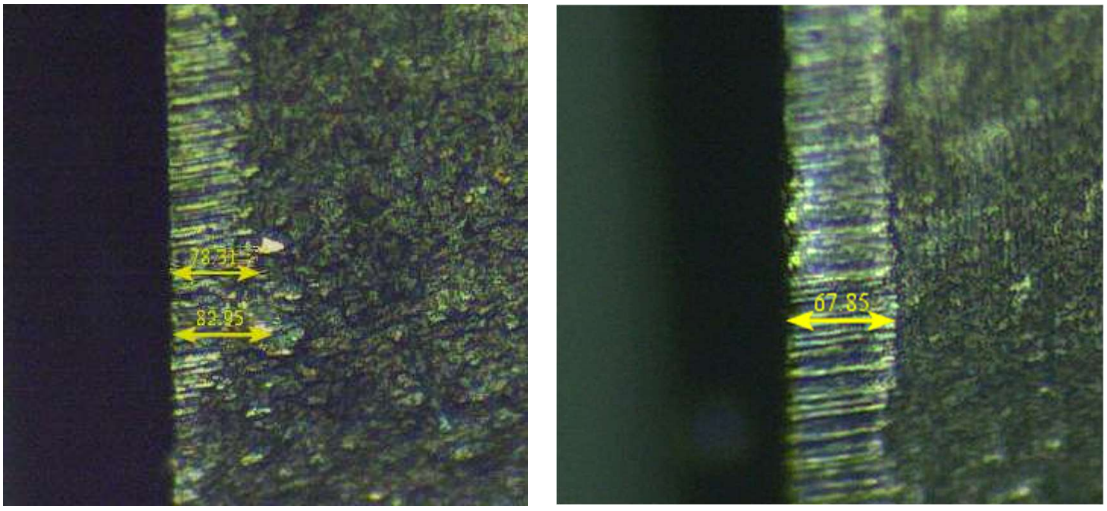

(**a**) (**b**)

Figure 6. The wear of BL (**a**) и BH (**b**) specimen at fine grinding of steel.

4. Discussion

At the sintering process, aluminum melts, and boron nitride powder partly dissolves in aluminum melt. Aluminum reacts with nitrogen [18], giving aluminum nitride (3), while boron atoms, been dissolved in aluminum melt, react with aluminum, giving aluminum borides (4):

$$BN_{(s)} + Al_{(l)} \rightarrow AlN_{(s)} + [B] \quad (3)$$

$$Al_{(l)} + 2[B] \rightarrow AlB_{2(s)} \quad (4)$$

There is a certain solubility limit for boron in liquid aluminum. The excess of boron reacts with aluminum to form AlB_2 и AlB_{12} [19]. Both reactions (3, 4) are possible at a temperature of 1450 °C.

The free Gibbs energy at 1700 K (1427 °C) for reaction (3) is −116,1 kJ/mol, and the value of free Gibb's energy for reaction (4) is −150 kJ/mol.

Yet we should remember that AlB_{12} is a high-temperature phase that transforms at cooling to low-temperature AlB_2. Different researchers [20,21] give temperatures from 956 °C to 1350 °C for the reaction (5):

$$5Al_{(l)} + AlB_{12(s)} \rightarrow 6AlB_{2(s)} \quad (5)$$

At cooling AlB_{12}, after the sintering process at multi-anvil compression conditions, reacts with molten aluminum and transforms to $AlB_{2(s)}$, that can be seen at XRD (Figure 1). These reactions (3–5) occur at sintering of BH and BL groups' specimens. There are no traces of unreacted aluminum on XR diffractograms, although the duration of the sintering process itself at temperatures 1400–1450 °C is only 5 min. Yet presumably, the reactions may proceed from the aluminium's melting point.

The summary reaction of boron nitride and aluminum may be written as:

$$2BN_{(s)} + 3Al_{(l)} \rightarrow 2AlN_{(s)} + AlB_{2(s)} \quad (6)$$

Titanium carbide TiC and titanium nitride TiN may slowly react with molten aluminum according to reactions:

$$Ti_xC_y + Al \rightarrow Ti_{1-x}C_{1-y} + TiAl \tag{7}$$

$$Ti_xC_y + Al \rightarrow Ti_{1-x}N_{1-y} + TiAl \tag{8}$$

Titanium atoms may dissolve in the molten aluminum. They may exist in solid solutions and form intermetallic compounds [22]. Their amount is small; they are not detected on diffractograms (Figure 1). The intervals of homogeneity of titanium carbide and titanium carbide are rather broad, so the amounts of TiN and TiC should remain almost unchanged.

There are two compounds—Mo_2B and MoB_2 in the system Mo-B [23]. However, there are no traces of these compounds on the diffractogram (Figure 1). According to EDX spectra, molybdenum may exist in cBN-based material in unreacted form (separate grains of molybdenum) and in the form of molybdenum borides (some part of molybdenum reacts with cBN). These compounds may appear only if there is sufficient solubility of molybdenum in molten aluminum, which doesn't occur. Also, there are no traces of molybdenum carbides.

As was said earlier, the process of sintering and consolidation of cBN-based materials is accompanied by reactions. These reactions proceed with volume transformations (volume effects). The reaction products may appear to have a negative volume transformation and a positive volume transformation. The volume transformations may affect the properties of materials.

In our case, we can neglect the volume transformations of reactions (7, 8). We are free not to take into account the reactions of molybdenum. The only chemical process that is necessary to take into account at the six-anvil HPHT process is the dissolution of cBN on molten aluminum and appearing of aluminum nitride AlN and aluminum boride AlB_2 according to reaction (6).

The mole volume is mole weight (gram) divided by density (gram/sm^3). The mole volume of reagents and reactants is:

$$Atomic\ volume\ of\ BN: \frac{24.81}{3.53} = 7.02, \tag{9}$$

$$Atomic\ volume\ of\ Al: \frac{26.98}{2.7} = 9.99, \tag{10}$$

$$Atomic\ volume\ of\ AlB_2: \frac{49}{3.19} = 15.36, \tag{11}$$

$$Atomic\ volume\ of\ AlN: \frac{41}{3.26} = 12.58. \tag{12}$$

Total volume changes in the course of the reaction (5) is calculated as:

$$\Delta V / V = (V(AlB_2) + 2V(AlN)) / (3V(Al) + 2V(BN)) = (15.36 + (2 \times 12.58)) / ((2 \times 7.02) + (3 \times 9.99)) = 0.92 \tag{13}$$

The mole volumes of final reactants AlB_2 and AlN are smaller than those of starting components cBN and aluminum. The volume changes due to volume transformations in a chemical reaction is 8%. The aluminum boride and aluminum nitride appear in smaller places, then start reagents such as cubic boron nitride and aluminum. We can suppose that this plays a positive role in all-direction anvil HPHT.

Two sets of cBN cutting tools with low and high cubic boron nitride were fabricated and investigated. The cutting tools demonstrated satisfactory results in finishing the grinding of hardened steels in industrial conditions.

5. Conclusions

At high-pressure high-temperature compaction of cubic boron nitride-based materials, the sintering additive aluminum plays two roles: it supports shrinkage at high pressures, promoting the sliding of grains of cBN. However, during compaction at high temperatures, aluminium reacts with cBN, titanium carbide and titanium nitride. In our experiments, there was no free aluminum in the final cBN materials of BH and BL groups.

The sintering and compaction of cubic boron nitride (cBN is followed by chemical reactions. The chemical reactions are accompanied by volume transformations (volume effects). The molecular volume of reaction products might be lower than that of starting substances, but it might be bigger.

The volume transformation (volume effect) of the main reaction of cBN with aluminum is negative. The value of the volume transformation is 8%, which may be considered positive in the case of six-anvil compaction.

The shrinkage of the BH group specimen, which has a lower cBN content and a higher reacting additive content, is 37.8%. The shrinkage of the specimen of BL group with a bigger content of cBN and smaller content of reacting additives is 32.2%, which can be explained by a bigger total volume change in the case of bigger content of reacting additives.

Acknowledgments

Authors are grateful to company "Microbor LLC" for experimental materials and for providing the equipment for the processing of the cutting tools.

Author Contributions

Conceptualization, A.Y. and M.A.; Methodology, A.Y., M.A.; Formal Analysis, M.A.; Investigation, S.P.; Resources, M.A.; Data Curation, M.A.; Writing—Original Draft Preparation, S.P. and A.Y.; Writing—Review & Editing, S.P. and A.Y.; Visualization, S.P.; Supervision, M.A.; Project Administration, M.A.

Ethics Statement

Not applicable.

Informed Consent Statement

Not applicable.

Funding

This research received no external funding.

Declaration of Competing Interest

The authors declare that they have no known competing financial interests or personal relationships that could have appeared to influence the work reported in this paper.

References

1. Sobiyi K, Sigalas I, Akdogan G, Turan Y. Performance of mixed ceramics and cBN tools during hard turning of martensitic stainless steel. *Int. J. Adv. Manuf. Technol.* **2014**, *77*, 861–871. doi:10.1007/s0070-014-6506-z.
2. *ISO16462:2014*; Cubic Boron Nitride Inserts, Tipped or Solid. Dimensions, Types. 2014. [Electronic resource]–Access mode. Available online: https://www.intechopen.com/online-first/significanceof-boron-nitride-in-composites-and-its-applications (accessed on 2 July 2024).
3. Bushlya V, Lenrick F, Stahl JE, Saoubi RM. Influence of oxygen on the tool wear in machining. *CIRP Ann.* **2018**, *67*, 79–82. doi:10.1016/j.cirp.2018.03.011.
4. Kanyanta V. *Microstructure–Property Correlations for Hard, Superhard, and Ultrahard Materials*; Springer: Cham, Switzerland, 2016. doi:10.1007/978-3-319-29291-5.
5. McKie A, Winzer J, Sigalas I, Herrmann M, Weiler L, Rodel J, et al. Mechanical properties of cBN-Al composite materials. *Ceram. Int.* **2021**, *37*, 1–8. doi:10.1016/j.ceramint.2010.07.034.
6. Angseryd J, Andren HO. An in-depth investigation of the cutting speed impact on the degraded microstructure of worn PcBN cutting tools. *Wear* **2011**, *271*, 2610–2618. doi:10.1016/j.wear.2010.11.059.
7. Zhang L, Lin F, Lv Z, Xu C, He X, Wang W, et al. cBN-Al-HfC composites: Sintering behaviors and mechanical properties under high pressure. *Int. J. Refract. Met. Hard Mater.* **2015**, *50*, 221–226. doi:10.1016/j.ijrmhm.2015.01.015.
8. Costes JP, Guillet Y, Poulachon G, Dessoly M. Tool-life and wear mechanisms of cBN tools in machining of Inconel 718. *Int. J. Mach. Tools Manuf.* **2007**, *47*, 1081–1087. doi:10.1016/j.ijmachtools.2006.09.031.

9. Xie X, Cao R, Zuo D, Lin Z. WC-Co-cBN composite hard alloy and preparation method thereof. Patent CN 107739950 B, 17 December 2019.
10. Benko E, Stanisław JS, Królicka B, Wyczesany A, Barr TL. cBN–TiN, cBN–TiC composites: Chemical equilibria, microstructure and hardness mechanical investigations, s.l. *Diam. Relat. Mater.* **1999**, *8*, 1838–1846.
11. Wu J, Wang H, Wang C, Tang Y, Hou Z, Wan S, et al. Ouyang, High pressure synthesis of tungsten carbide–cubic boron nitride (WC–cBN) composites: Effect of thermodynamic condition and cBN volume fraction on their microstructure and properties. *J. Eur. Ceram. Soc.* **2022**, *42*, 4503–4512. doi:10.1016/j.jeurceramsoc.2022.04.037.
12. Can N, Andersin SA. Cubic boron nitride compact. Patent U.S. 8,007,552 B2, 30 August 2011.
13. *ISO5017:2013-01*; Dense Shaped Refractory Products—Determination of Bulk Density, Apparent Porosity and True Porosity. International Organization for standardization: Geneva, Switzerland, 2013.
14. Niihara K, Morena R, Hasselman DPH. Evaluation of KIC of Brittle Solids by the Indentation Method with Low Crack-To-Indent Ration. *J. Mater. Sci.* **1982**, *1*, 13–16.
15. Lawn BR, Fuller ER. Equilibrium penny-like cracks in indentation fracture. *J. Mater. Sci.* **1975**, *10*, 2016–2024. doi:10.1007/BF00557479.
16. Tanaka K. Elastic/plastic indentation hardness and indentation fracture toughness: The inclusion core model. *J. Mater. Sci.* **1987**, *22*, 1501–1508.
17. Durst K, Backes B, Franke O, Göken M. Indentation size effect in metallic materials: Modeling strength from pop-in to macroscopic hardness using geometrically necessary dislocations. *Acta Mater.* **2006**, *54*, 2547–2555. doi:10.1016/j.actamat.2006.01.036.
18. Li Y, Kou Z, Wang H, Wang K, Tang H, Wang Y, et al. High pressure sintering behavior and mechanical properties of cBN-Ti_3Al and cBN-Ti_3Al-Al composite materials. *High Press. Res.* **2012**, *34*, 524–531. doi:10.1080/08957959.2012.736507.
19. Hall A, Economy J. The Al (L)+ AlB12↔ AlB2 peritectic transformation and its role in the formation of high aspect ratio AlB2 flakes. *Phase Equilib.* **2000**, *20*, 63–69.
20. Sigworth GK. The grain refining of aluminum and phase relationships in the Al-Ti-B system. *Metall. Trans. A* **1984**, *15*, 277–282.
21. Rogl P, Schuster JC. *Phase Diagrams of Ternary Boron Nitride and Silicon Nitride System*; ASM International: Almere, the Netherlands, 1992.
22. Liu Y, Zhang W, Peng Y, Fan G, Liu B. Effects of Ti-Al Alloy as a Binder on Cubic Boron Nitride Composites. *Materials* **2021**, *21*, 6335. doi:10.3390/ma14216335.
23. Lyakishev NP. Phase Diagrams of Binary Metallic Systems, Mashinostroenie. *Moscow* **1996**, *1*, 461–464.